International Journal of Electronics

ISSN: 0020-7217 (Print) 1362-3060 (Online) Journal homepage: http://www.tandfonline.com/loi/tetn20

High-efficiency resonant coupled wireless power transfer via tunable impedance matching

Tanbir Ibne Anowar, Surajit Das Barman, Ahmed Wasif Reza & Narendra Kumar

To cite this article: Tanbir Ibne Anowar, Surajit Das Barman, Ahmed Wasif Reza & Narendra Kumar (2017) High-efficiency resonant coupled wireless power transfer via tunable impedance matching, International Journal of Electronics, 104:10, 1607-1625, DOI: 10.1080/00207217.2017.1312711

To link to this article: http://dx.doi.org/10.1080/00207217.2017.1312711

Accepted author version posted online: 27 Mar 2017.
Published online: 21 Apr 2017.

INTERNATIONAL JOURNAL OF ELECTRONICS, 2017
VOL. 104, NO. 10, 1607–1625
https://doi.org/10.1080/00207217.2017.1312711

High-efficiency resonant coupled wireless power transfer via tunable impedance matching

Tanbir Ibne Anowar[a], Surajit Das Barman[a], Ahmed Wasif Reza[b] and Narendra Kumar[a]

[a]Department of Electrical Engineering, Faculty of Engineering, University of Malaya, Kuala Lumpur, Malaysia; [b]Department of Computer Science and Engineering, Faculty of Science and Engineering, East West University, Dhaka, Bangladesh

ABSTRACT

For magnetic resonant coupled wireless power transfer (WPT), the axial movement of near-field coupled coils adversely degrades the power transfer efficiency (PTE) of the system and often creates sub-resonance. This paper presents a tunable impedance matching technique based on optimum coupling tuning to enhance the efficiency of resonant coupled WPT system. The optimum power transfer model is analysed from equivalent circuit model via reflected load principle, and the adequate matching are achieved through the optimum tuning of coupling coefficients at both the transmitting and receiving end of the system. Both simulations and experiments are performed to evaluate the theoretical model of the proposed matching technique, and results in a PTE over 80% at close coil proximity without shifting the original resonant frequency. Compared to the fixed coupled WPT, the extracted efficiency shows 15.1% and 19.9% improvements at the centre-to-centre misalignment of 10 and 70 cm, respectively. Applying this technique, the extracted S_{21} parameter shows more than 10 dB improvements at both strong and weak couplings. Through the developed model, the optimum coupling tuning also significantly improves the performance over matching techniques using frequency tracking and tunable matching circuits.

ARTICLE HISTORY
Received 9 May 2016
Accepted 5 February 2017

KEYWORDS
Wireless power transfer; magnetic resonance coupling; power transfer efficiency; optimum coupling tuning; impedance matching; frequency splitting

1. Introduction

With the rapid evolvement of portable consumer appliances, wireless power transfer (WPT) is now being the top research interest complementing wide variety of applications including charging of biomedical implant sensors (Hao et al., 2013; RamRakhyani, Mirabbasi, & Mu, 2011), batteries (Moon et al., 2015; Yoon, Nam, & Cho, 2016) and portable electronic devices (Jabbar, Song, & Jeong, 2010; Sample, Meyer, & Smith, 2011), powering of home appliances (Hatanaka et al., 2002; Yungtaek & Jovanovic, 2003) and high-power electric vehicles (Choi, Gu, Jeong, & Rim, 2015; Jang, Suh, & Kim, 2016; Sallan, Villa, Llombart, & Sanz, 2009), etc. The concept of remote charging in the absence of conducting wires ensures a reliable, cost-effective and safe use of the devices. In the early twenty-first century, the prominent and efficient WPT technologies for consumer applications were the inductive power transfer (IPT) (Casanova, Zhen Ning, & Jenshan, 2009; Madawala & Thrimawithana, 2011; Wang et al., 2016; Wei, Siu-Chung, Tse, & Qianhong, 2014; Zhen Ning, Chinga, Ryan, & Jenshan, 2009) and microwave power transfer

CONTACT Ahmed Wasif Reza wasif@ewubd.edu Department of Computer Science and Engineering, Faculty of Science and Engineering, East West University, Dhaka, Bangladesh

Present affiliation for Surajit Das Barman is Department of Computer Science and Engineering, Faculty of Science and Engineering, East West University, Dhaka, Bangladesh

(MPT) (Abbasi, Atif Adnan, Amin, & Kamran, 2009, January; Benford, 2008; Brown & Eves, 1992). The IPT technique adapting electromagnetic (EM) induction is only effective for wireless charging within a short operating range. On the other hand, the EM radiation-based MPT system poorly suffers to maintain line-of-sight connection due to its omnidirectional properties. Also, the energy transmission range of MPT lies out of the IEEE standard for radio frequency (RF) EM fields (IEEE Standard, 2006, April). The conceivable development of wireless powering occurred after the demonstration of strong magnetic resonant coupling-based WPT on 2007 (Karalis, Joannopoulos, & Soljačić, 2008; Kurs et al., 2007) and has recently been demonstrated experimentally (Barman et al., 2015; Chen, Chu, Lin, & Jou, 2010; Dukju & Songcheol, 2013a, 2014; Kurs et al., 2007; Park et al., 2014; Ricketts, Chabalko, & Hillenius, 2013a; Sample et al., 2011) to extend their power transfer to a more convenient midrange distance.

Nevertheless, the received power level in resonant coupled WPT is highly sensitive to coil movement and alignment. Any change in the optimal position between the transmitting (TX) and receiving (RX) coils affects the overall circuit impedance which often splits the operating frequency and degrades the power transfer efficiency (PTE) of the WPT system (Dukju & Songcheol, 2013a; Imura & Hori, 2011; Sample et al., 2011; Yiming, Zhengming, & Kainan, 2014). Therefore, the consideration of optimum PTE over large coupling distance is required to establish a practical WPT system. Also, the aim of improving power transmission to the load in terms of transfer efficiency is important prior to design any low-power RF circuits where system's efficiency is not the main interest. In such case, maximum power transfer principle based on impedance matching is suitable to design low-power wireless powering applications with extended operating range (Barman et al., 2015).

Several techniques have been discussed before to achieve optimum efficiency for resonant coupled WPT system. To overcome the frequency splitting, the optimum frequency tracking has been proposed (Dukju & Songcheol, 2013b; Sample et al., 2011); however, these methods use a rather wide frequency band and often violates the industrial, scientific and medical regulation standard. Also, it is inconvenient to adjusting the source frequency by manual coarse tuning in most engineering applications. Several adaptive impedance matching using tunable lossy matching circuits has been studied (Barman, Reza, Kumar, & Anowar, 2016; Teck Chuan, Kato, Imura, Sehoon, & Hori, 2013; Waters, Sample, & Smith, 2012, August), but the integration of varactors limits the range of tuning to obtain optimal efficiency. The reported works in Kim, Choi and Jeong (2013), Nair and Choi (2016), Park and Lee (2014) detail maximising efficiency using multiple loop coils; however, these techniques require manual coarse switching of appropriate loop coils connected with external capacitor respective to the amount of TX–RX coupling. Various adaptive matching employing capacitor matrix are also discussed in Chen et al. (2010), Lu and Nguang (2015), Ricketts, Chabalko and Hillenius (2013b) to adjust the operating frequency and improve the power transfer capability, but most of these methods are time consuming and require complex capacitive tuning to maintain resonance at close coil proximity.

This paper presents a tunable impedance matching technique based on optimum coupling tuning to optimise the transfer efficiency of resonant coupled WPT system over a wide operational range. The optimum power transfer model of the resonant coupled system is analysed from an equivalent circuit model of magnetically coupled coil configuration using reflected load principle (Kiani & Ghovanloo, 2012), and the adequate matching is achieved through the optimum adjustment and tuning of coupling coefficients at both the TX and RX sides. Empirical equations for the optimum couplings and maximum PTE are derived as a function of loaded Q-factor and coupling between the intermediate coupled coil pairs. An experimental set-up has been established to evaluate the model parameters and efficiency, which are in turn justified with the analytical model.

The paper is organised as follows. Section 2 includes the analysis of the power transfer model of four-coil resonant coupled WPT system. The optimum coupling equations for impedance matching to optimise PTE is formulated in Section 3. Section 4 discusses the simulation and experimental results, followed by the conclusion in Section 5.

2. Power transfer model of resonant coupled WPT

In contrary to the conventional two-coil inductive link system, the resonant coupled system typically depends on four-coil system, which exhibits high efficiency even in far-field condition. The model of resonant coupled WPT shown in Figure 1 consists of two loop coils (source and load coils) and two multi-turn planar spiral coils (TX and RX coils) placed on intermediate position between the loop coils. Generally, the loop coils are used for impedance matching mechanism, and made of single or two turns having external capacitors connected in series with each. This structure makes them resonate at the identical frequency of the intermediate coils for maximum power transfer.

A signal generator is used to generate an oscillating sinusoidal wave at the frequency of interest. To amplify the signal strength, the oscillating signal is then passed through an RF amplifier before feeding onto the source and TX coils. When all the coils are tuned at the same frequency, the RX and load coils induced adequate magnetic field to provide sufficient energy in the load. Because of large Q-factor of both TX and RX coils, the key aspect in transfer efficiency practically depends on the distance (d_{TR}) between them and also helps to overcome the low magnetic couplings among the coils. Here, d_{ST}(d_{RD}) represents the distance between the source and TX coils (load and RX coils). As the energy transferred per cycle is dependent on the amount of coupling, the system needs to be optimised for having maximum efficiency at a defined operating point.

To analyse the power transfer model of the resonant coupled system, the planar spiral form of the coupled coils based on lumped parameters (Figure 2(a)) are considered as its efficiency is less affected by the coil distance variation. The series compensated electrical model representation of the 4-coil system is illustrated in Figure 2(b). Here, L_S and L_D represent the self-inductance of the source and load coils, respectively, and R_{PS} and R_{PD} are the corresponding parasitic resistances. Both coils are enclosed in series with respective compensated capacitors C_S and C_D to maintain resonance even at variable load conditions. The TX coil is modelled as a multi-turn planar spiral resonator of self-inductance L_T with parasitic resistance R_{PT} and parasitic capacitance C_T. Similarly, the RX coil is represented by L_R, R_{PR} and C_R, respectively. An oscillating field generally produces current I_S in the source coil when excites from the sinusoidal voltage source of amplitude V_G and internal resistance (R_G). Here, V_{in} represents the input voltage between the voltage source and input port of the source coil. When the operating frequency of V_G is equal to the resonant frequency, the coil current becomes maximum to transmit energy mostly to the RX and load coils. The direct coupling coefficients between each of the two adjacent magnetically coupled coils are k_{ST}, k_{TR} and k_{RD}. The weak cross-coupling coefficients between the source and RX coils (k_{SR}), the

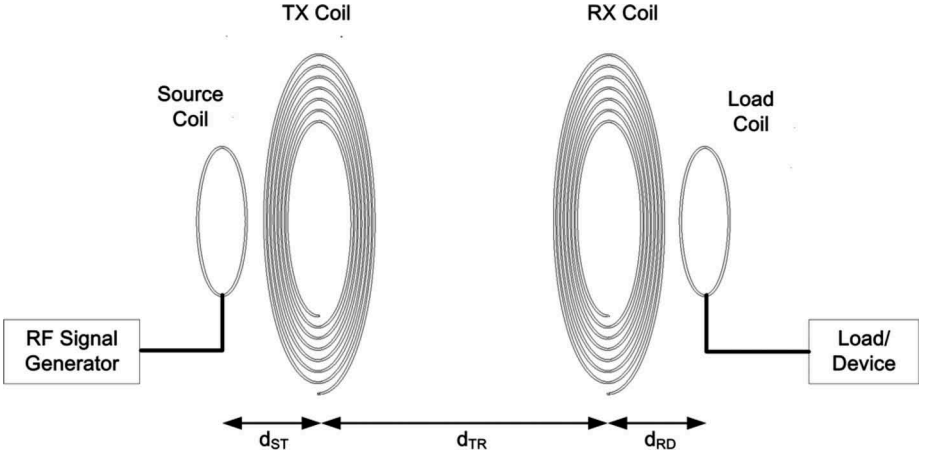

Figure 1. WPT system using magnetic resonant coupled coils.

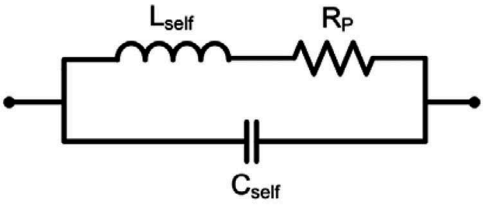

(a)

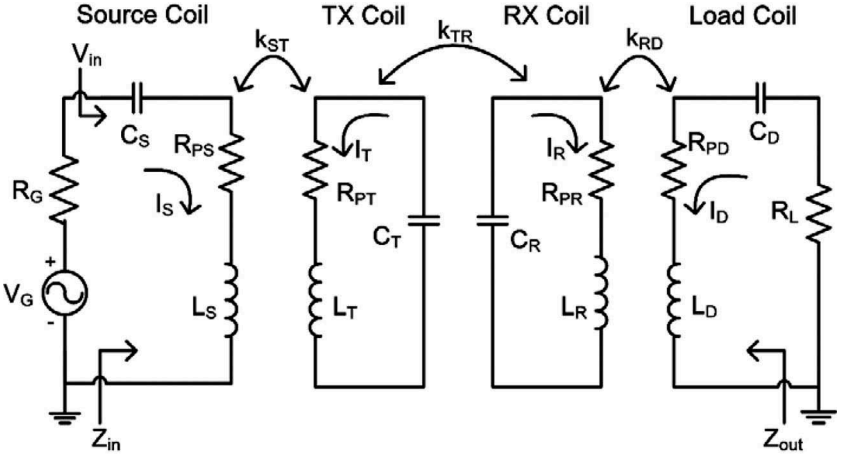

(b)

Figure 2. Equivalent electrical model representation of the (a) circular coil and (b) four-coil resonant coupled WPT system.

TX and load coils (k_{TD}), and the source and load coils (k_{SD}) are neglected in the analysis. Theoretically, the coupling coefficients are in the range of 0–1 and can be calculated as

$$k_{ab} = \frac{M_{ab}}{\sqrt{L_a L_b}}; (\text{Here, } a, b = 1, 2, 3, \ldots\ldots, n), \tag{1}$$

where M_{ab} represents the mutual inductance between two coils, which can be expressed as Neumann form (Terman, 1943) given as

$$M_{ab} \cong \frac{\pi\mu N_a N_b r_a^2 r_b^2}{2\left(d_{ab}^2 + r_b^2\right)^{\frac{3}{2}}}. \tag{2}$$

If the resonant frequencies of all coils are the same, then it could be deduced that

$$j\omega_0 L_S + \frac{1}{j\omega_0 C_S} = j\omega_0 L_T + \frac{1}{j\omega_0 C_T} = j\omega_0 L_R + \frac{1}{j\omega_0 C_R} = j\omega_0 L_D + \frac{1}{j\omega_0 C_D} = 0. \tag{3}$$

Here, ω_0 is the self-resonant frequency of the individual coil. Therefore, $Q_i = \frac{\omega_0 L_i}{R_i} = \frac{1}{\omega_0 C_i R_i} = \frac{1}{R_i}\sqrt{\frac{L_i}{R_i}}$ represents the Q-factor of the i^{th} coil. By using the reflected load principles, the reflected impedances at the resonant frequency can be, respectively, written as

$$Z_{eqRD} == \frac{(\omega_0 M_{RD})^2}{R_{PD}+R_L} = \frac{\omega_0^2 k_{RD}^2 L_R L_D}{R_{PD}+R_L} \tag{4}$$

$$Z_{eqTR} = \frac{\omega_0^2 k_{TR}^2 L_T L_R}{R_{PR}+Z_{eqRD}} = R_{PT}\left(\frac{k_{TR}^2 Q_T Q_R}{1+k_{RD}^2 Q_R Q_D}\right) \tag{5}$$

$$Z_{eqST} = (R_G+R_{PS})\left(\frac{k_{ST}^2 Q_S Q_T (1+k_{RD}^2 Q_R Q_D)}{1+k_{TR}^2 Q_T Q_R + k_{RD}^2 Q_R Q_D}\right), \tag{6}$$

where Z_{eqRD}, Z_{eqTR} and Z_{eqST} represent the reflected impedance from load to RX coil, from RX to TX coil and from TX to source coil, respectively, as shown in Figure 3. Subsequently, the transfer efficiency of individual coil can be simply derived as

$$\eta_D = \frac{I_D^2 R_L}{I_D^2 (R_{PD}+R_L)} = \frac{R_L}{R_{PD}+R_L} \tag{7}$$

$$\eta_R = \frac{Z_{eqRD}}{R_{PR}+Z_{eqRD}} = \frac{k_{RD}^2 Q_R Q_D}{1+k_{RD}^2 Q_R Q_D} \tag{8}$$

$$\eta_T = \frac{Z_{eqTR}}{R_{PT}+Z_{eqTR}} = \frac{k_{TR}^2 Q_T Q_R}{1+k_{TR}^2 Q_T Q_R + k_{RD}^2 Q_R Q_D} \tag{9}$$

$$\eta_S = \frac{Z_{eqST}}{R_{PS}+Z_{eqST}}. \tag{10}$$

Now, the overall PTE of the resonant coupled WPT can be stated as the product of the four sub-efficiencies given as

$$\begin{aligned}\eta_{PTE} &= \eta_S \eta_T \eta_R \eta_D \\ &= \left[\left(\frac{Z_{eqST}}{R_{PS}+Z_{eqST}}\right)\left(\frac{k_{TR}^2 Q_T Q_R}{1+k_{TR}^2 Q_T Q_R + k_{RD}^2 Q_R Q_D}\right)\left(\frac{k_{RD}^2 Q_R Q_D}{1+k_{RD}^2 Q_R Q_D}\right)\left(\frac{R_L}{R_{PD}+R_L}\right)\right].\end{aligned} \tag{11}$$

To analyse the figure of merit of the resonant coupled system, the forward wave transmission ratio S_{21} parameter can be used. Generally, S_{21} defines the power gain of the system which is calculated to be

$$S_{21} = 2\frac{V_L}{V_G}\sqrt{\frac{R_G}{R_L}}. \tag{12}$$

The voltage across the load is $V_L = -I_D R_L$. To compute I_D, Kirchhoff's voltage law is employed to the circuit in Figure 2(b). The governing equations can be written in matrix form as follows

$$\begin{bmatrix} Z_S' & k_{ST}a_{ST} & 0 & 0 \\ k_{ST}a_{ST}^{-1} & Z_T' & k_{TR}a_{TR} & 0 \\ 0 & k_{TR}a_{TR}^{-1} & Z_R' & k_{RD}a_{RD} \\ 0 & 0 & k_{RD}a_{RD}^{-1} & Z_D' \end{bmatrix} \begin{bmatrix} I_S \\ I_T \\ I_R \\ I_D \end{bmatrix} = \begin{bmatrix} \frac{V_G}{j\omega_0 L_S} \\ 0 \\ 0 \\ 0 \end{bmatrix}. \tag{13}$$

Here, $Z_X' = \frac{R_X}{j\omega_0 L_X}$ represents the transformed impedance of each coil. The inductor factor is defined as $a_{XY} = \sqrt{L_Y/L_X}$. Therefore, the current I_D in the load coil can be simplified from Equation (13) in employing the substitution method

$$I_D = \frac{k_{ST}k_{TR}k_{RD}Q_T Q_R \sqrt{Q_S Q_D}\,\frac{jV_G}{\sqrt{(R_G+R_{PS})(R_{PD}+R_L)}}}{1+k_{ST}^2 Q_S Q_T + k_{TR}^2 Q_T Q_R + k_{RD}^2 Q_R Q_D + k_{ST}^2 k_{RD}^2 Q_S Q_T Q_R Q_D}. \tag{14}$$

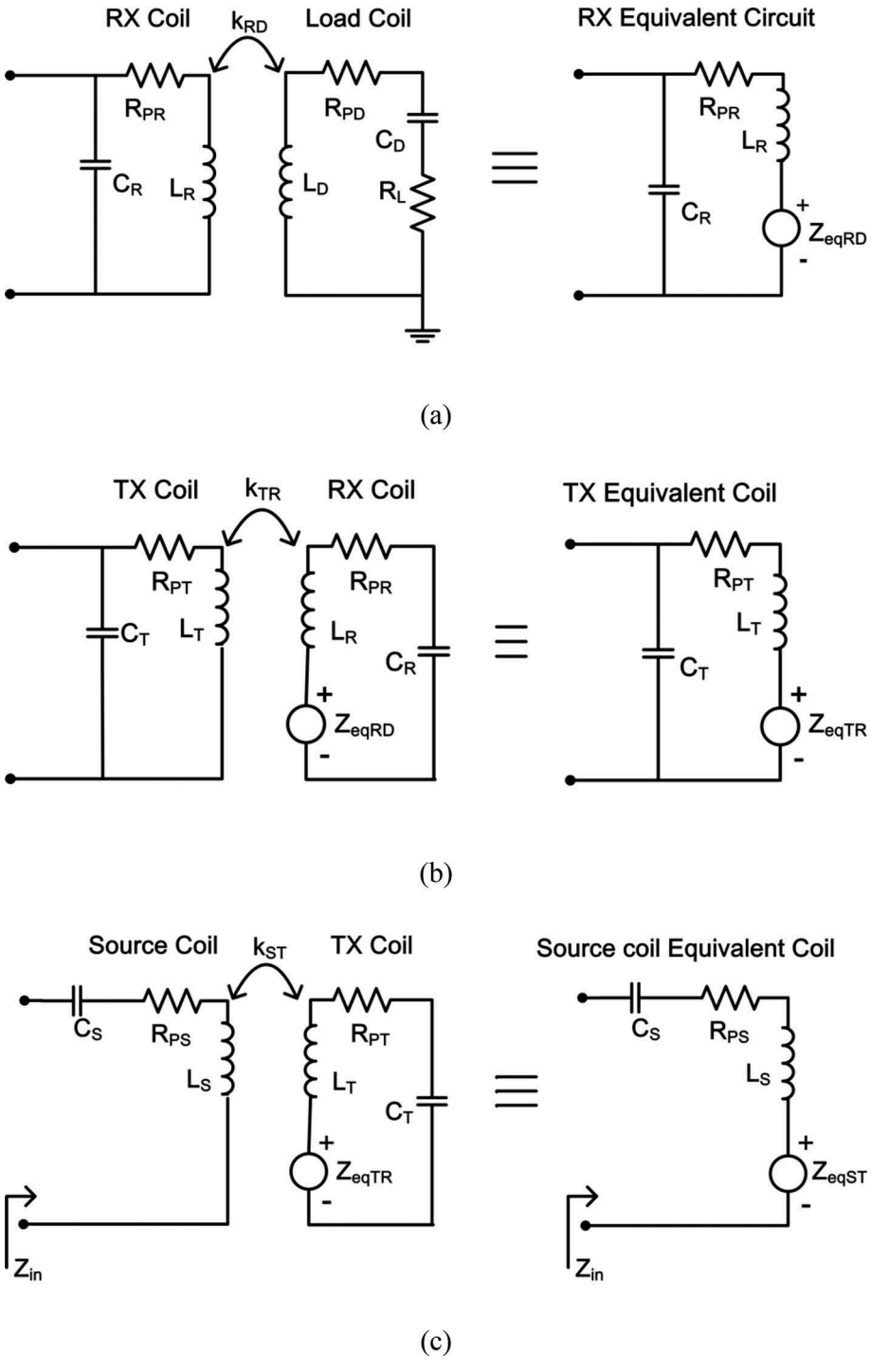

Figure 3. Simplified circuit model of four-coil system with compensation sources representing reflected load (a) from load to RX coil, (b) from RX to TX coil and (c) from TX to source coil.

From Equations (12) and (14), the magnitude of S_{21} is obtained as

$$|S_{21}| = \left(\frac{2k_{ST}k_{TR}k_{RD}Q_TQ_R\sqrt{Q_SQ_D}}{(1+k_{ST}^2Q_SQ_T)(1+k_{RD}^2Q_RQ_D)+k_{TR}^2Q_TQ_R}\right)\left(\sqrt{\frac{R_GR_L}{(R_G+R_{PS})(R_{PD}+R_L)}}\right). \quad (15)$$

3. Impedance matching to optimise PTE

Typically, the coupling coefficients k_{ST} and k_{RD} are kept constant in the conventional fixed coupled WPT, where the system's voltage transfer function is strongly dependent on the coupling k_{TR}. Therefore, the overall circuit impedance is greatly affected by the distance d_{TR} which in turn lowers the efficiency and often creates sub-resonances. To improve the PTE, the input impedance Z_{in} and output impedance Z_{out} of the system need to be a conjugate match with the optimal source and load impedances. This required matching can be achieved by the optimum tuning of coupling coefficient k_{ST} and k_{RD}, respectively, which are visualised as two equivalent T-matching networks of the system as illustrated in Figure 4.

As observed in Figure 4, the equivalent matching network A is the combination of the source and TX coils, and can be envisaged as a T-equivalent circuit consisting of C_S, L_S, C_T and the coupling coefficient k_{ST}. Similarly, C_R, L_D, C_D and the coupling coefficient k_{RD} form the equivalent matching network B which is the combination of the RX and load coils. Here, the magnetising inductance $M_{ST}(M_{RD})$ represents the extent of optimum magnetic flux linkage between the source and TX coils (RX and load coils), which is a function of the optimum value of $k_{ST}(k_{RD})$. Therefore, the self-inductance of the conventional source (load) coil can be defined as the combination of the leakage inductance $L_S - M_{ST}$ $(L_R - M_{RD})$ and the magnetising inductance $M_{ST}(M_{RD})$. Among the efficiency described in Equation (11), the source coil efficiency η_S and load coil efficiency η_D are almost constant as they are directly dependent on the optimal value of the source resistance R_G and load resistance R_L, respectively. Generally, the parasitic resistance of the source and load coils are much smaller than R_G and R_L, that is, $R_{PS} << R_G$ and $R_{PD} << R_L$ approximates both the η_S and η_D in Equation (11) equal to 1. It means, the actual system's performance is a dependent function of the product of TX coil efficiency η_T and RX coil efficiency η_R. Therefore, maximising the product of η_T and η_R will lead the overall PTE of the system to be maximised.

$$\begin{aligned}\eta_{PTE} &= \left[\left(\frac{Z_{eqST}}{R_{PS}+Z_{eqST}}\right)\left(\frac{k_{TR}^2Q_TQ_R}{1+k_{TR}^2Q_TQ_R+k_{RD}^2Q_RQ_D}\right)\left(\frac{k_{RD}^2Q_RQ_D}{1+k_{RD}^2Q_RQ_D}\right)\left(\frac{R_L}{R_{PD}+R_L}\right)\right] \\ &= \left[\left(\frac{Z_{eqST}}{R_{PS}+Z_{eqST}}\right).\eta.\left(\frac{R_L}{R_{PD}+R_L}\right)\right],\end{aligned} \quad (16)$$

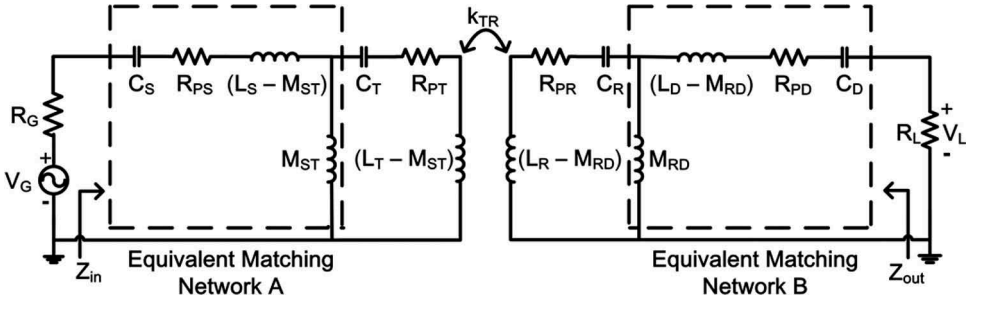

Figure 4. Equivalent circuit schematic of the tunable impedance matching approach. (Here, $M_{ST} = k_{ST(opt)}\sqrt{L_SL_T}$ and $M_{RD} = k_{RD(opt)}\sqrt{L_RL_D}$).

where, it is assumed $\left(\frac{k_{TR}^2 Q_T Q_R}{1+k_{TR}^2 Q_T Q_R + k_{RD}^2 Q_R Q_D}\right)\left(\frac{k_{RD}^2 Q_R Q_D}{1+k_{RD}^2 Q_R Q_D}\right) = \eta_T \eta_R = \eta$.

If the impedance ratio in Equation (15) is also approximated as 1, the expression of $|S_{21}|$ can be further simplified as

$$|S_{21}| \cong \frac{2k_{ST}k_{TR}k_{RD}Q_T Q_R\sqrt{Q_S Q_D}}{(1+k_{ST}^2 Q_S Q_T)(1+k_{RD}^2 Q_R Q_D)+k_{TR}^2 Q_T Q_R}. \tag{17}$$

In compliance to the principle of maximum power transfer, the matching network B acts to satisfy $Z_{out} = R_L^*$, where Z_{out} is a function of the power transferred to load. Hence, a derivative of the product η with respect to $\Delta_L = k_{RD}^2 Q_R Q_D$ is accounted and equating resultant to zero, yielding,

$$\frac{\partial}{\partial \Delta_L}(\eta) = 0. \tag{18}$$

Here, the product $\Delta_L = k_{RD}^2 Q_R Q_D$ acts as the matching factor between the RX and load coils. From the derivation of Equation (18), the matching condition to satisfy $Z_{out} = R_L^*$ can be extracted as

$$k_{RD}^2 Q_R Q_D = \left(1 + k_{TR}^2 Q_T Q_R\right)^{\frac{1}{2}}. \tag{19}$$

Therefore, the optimum coupling coefficient between the RX and load coils for maximum PTE is given as

$$k_{RD(opt)} = \frac{1}{\sqrt{Q_R Q_D}}\left(1 + k_{TR}^2 Q_T Q_R\right)^{\frac{1}{4}}. \tag{20}$$

Also, the output impedance Z_{out} from the solution of Equation (19) can be expressed as

$$Z_{out} = \omega_0 L_D\left(\frac{k_{RD}^2 Q_R}{\left(1 + k_{TR}^2 Q_T Q_R\right)^{\frac{1}{2}}}\right) - R_{PD}. \tag{21}$$

Similarly, the equivalent matching network A of the source and TX coils serves to satisfy $Z_{in} = R_G^*$ which results the input impedance Z_{in} as

$$\begin{aligned} Z_{in} &= R_G = R_{PS} + Z_{eqST} \\ &= R_{PS} + (R_G + R_{PS})\left(\frac{k_{ST}^2 Q_S Q_T(1 + k_{RD}^2 Q_R Q_D)}{1 + k_{TR}^2 Q_T Q_R + k_{RD}^2 Q_R Q_D}\right). \end{aligned} \tag{22}$$

Thus, from Equation (22), the optimum coupling between the source and TX coils to ensure maximum PTE can be derived as

$$k_{ST(opt)} = \sqrt{\frac{1}{Q_S Q_T}\left(\frac{R_G - R_{PS}}{R_G + R_{PS}}\right)}\left(1 + k_{TR}^2 Q_T Q_R\right)^{\frac{1}{4}}. \tag{23}$$

The theoretical accuracy of Equations (20) and (23) in case of matching at both sides of the WPT is explained in Appendix. Substituting the value of Equations (20) and (23) in both Equations (16) and (17), the maximum PTE of the resonant coupled WPT system can be approximated as

$$\eta_{(PTE)\max} = \left(\frac{Z_{eqST}}{R_{PS} + Z_{eqST}}\right)\left(\frac{k_{TR}^2 Q_T Q_R}{\left[1 + \left(1 + k_{TR}^2 Q_T Q_R\right)^{\frac{1}{2}}\right]^2}\right)\left(\frac{R_L}{R_{PD} + R_L}\right) \cong |S_{21}|^2. \tag{24}$$

The expression in Equation (24) reveals that the maximum transfer efficiency is heavily proportional to the product $k_{TR}^2 Q_T Q_R$ and approximately equal to the square of $|S_{21}|$, that is, the resonant coupled WPT with the proposed tunable matching acts like a two-port network. Compared to the

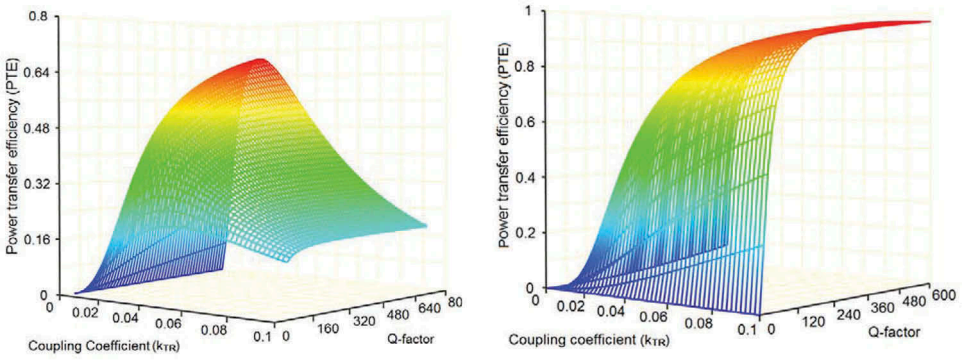

Figure 5. Power transfer efficiency versus coupling coefficient (k_{TR}) and Q-factor of resonant coupled WPT system at both (a) fixed couplings (with assuming $k_{ST} = 0.137$, $k_{RD} = 0.139$, $Q_{(loop-res)} = Q_S = Q_D = 2.63$) and (b) optimum couplings.

fixed coupled WPT, Figure 5 graphically validates the improvement in efficiency using impedance matching through optimum coupling tuning along with the significant extend of the operating range. In this paper, the proposed tunable matching is experimentally achieved by the adjustment of the distance d_{ST} and d_{RD} between the loop and intermediate coils according to the corresponding optimum value of k_{ST} and k_{RD}.

4. Simulation and experimental validation

Figure 6 shows the designed WPT system having four coils used to validate the theoretical model of the proposed matching technique. Copper wire having 1.4 mm of diameter is used to fabricate the coils. Both the source and load coils are built as loop resonator with two turns having 15 cm of outer diameter and 0.25 cm of pitch distance. The TX coil is a planar spiral type having outer diameter of 29 cm and winds up to 6.5 turns approximately in inward direction with a pitch of 1 cm. The RX coil is also designed carefully as symmetrical as TX to achieve equal resonant frequencies and high Q-factor. The structural design parameters of the fabricated coils and loops are given in Table 1.

The measurement of the coil parameters is done by Vector Network Analyzer (VNA) shown in Figure 6(a) because it is not always to find LCR meter for high-frequency range. The loop coils are connected to the VNA ports through SubMiniature version A (SMA) cables and connectors. One of the consequential challenges during the fabrication and assessment is to accurately measure the resonant frequency of the coils. Also, it is difficult to predict the coil's parasitic capacitance. Therefore, the spiral coils are manually trimmed at the end to tune the resonant frequency. With inherent self-inductance and parasitic capacitance of TX and RX coils, the resonant frequency of 17.1 MHz was determined experimentally. Besides this, RF Mica capacitors with low equivalent series resistance (ESR) value are coupled in series with each loop coil to resonate them at 17.1 MHz. Due to high series resistance, the Q-factor of each loop coil becomes limited at the exact operating frequency. The measured Q-factor of source and load coils with 50 Ω loading are 3.074 and 3.037, respectively. Under no-load condition, the measured peak-to-peak input voltage V_{in} is 19.2 V which should be half of the signal generator voltage V_G. A summary of the extracted parameters for each individual coil is given in Table 2.

To find the mutual coupling k_{TR} between the TX and RX coils, the coupling distance d_{TR} is swept over 10–85 cm by aligning all the coils in coaxial and series-aiding series-opposing method is employed via VNA. Figure 7 shows the extracted values of k_{TR} compared to the calculated values

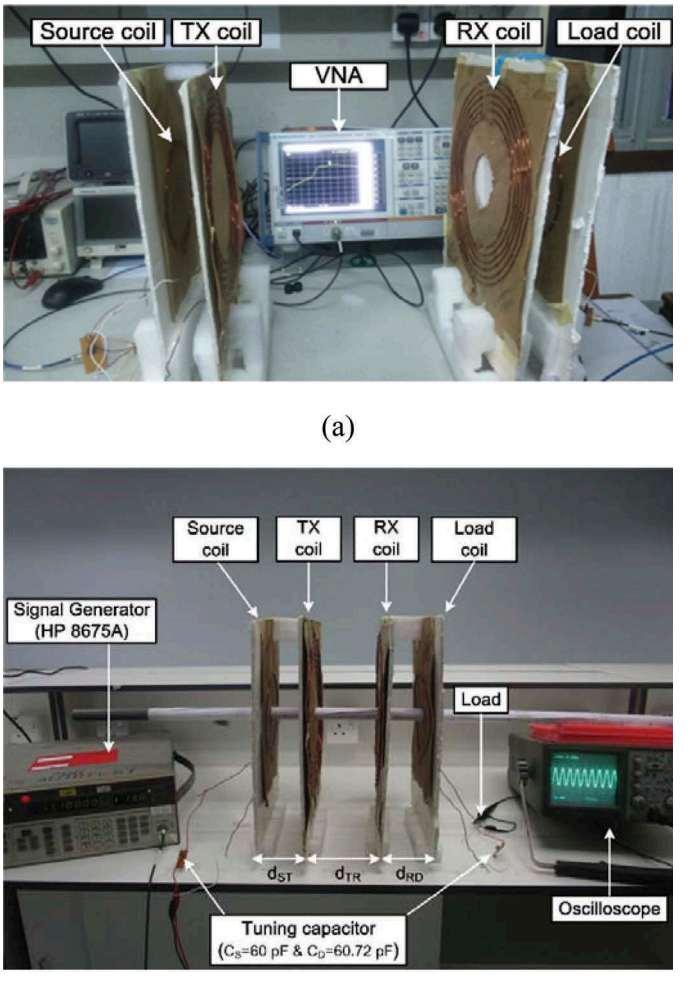

Figure 6. WPT prototype with resonant coupled coils: (a) mutual inductance measurement with VNA and (b) experimental set-up with optimum coupling tuning.

Table 1. Structural dimensions of the fabricated coils and loops.

	Values			
Design parameters	Source coil	TX coil	RX coil	Load coil
No. of turns (*N*)	2	6.5	6.5	2
Outer diameter (cm)	15	29	29	15
Pitch (cm)	0.25	1	1	0.25
Mean diameter (cm)	14.5	23.5	23.5	14.5
Wire diameter (mm)	1.4	1.4	1.4	1.4

deduced from Equations (1) and (2) using the measured value of coil parameters as given in the Table 2. To testify the effect of the tunable matching technique, an equivalent model of the resonant coupled WPT is established in Agilent ADS simulator, which incorporates the coil parameters in Table 2, computed k_{TR} and Equations (3)–(24). The proposed technique for improved PTE is also verified through measurement (Figure 6(b)) at which the coupling distance d_{TR} is increased in a step of 5 cm from 10 to 85 cm.

Table 2. Extracted lumped parameter values to represent circuit model for each individual coil.

Extracted parameters	Values			
	Source coil	TX coil	RX coil	Load coil
Inductance (μH)	1.444	13.185	13.386	1.4266
Parasitic resistance (Ω)	0.465	1.55	1.56	0.458
Capacitance (pF)	60	6.56	6.4	60.72
Resonant frequency (MHz)	17.09	17.11	17.19	17.1
Input voltage V_{in} (V)	19.2 (peak to peak)			

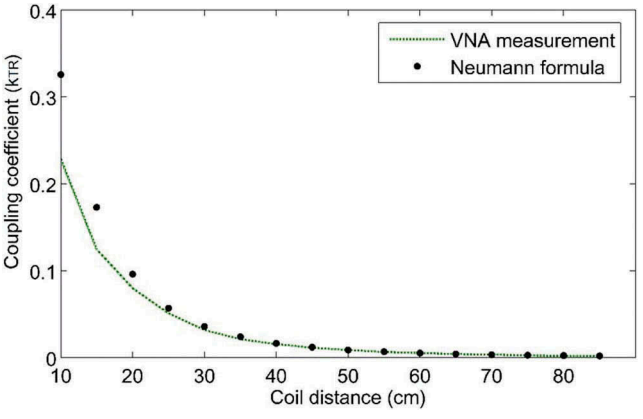

Figure 7. Mutual coupling (k_{TR}) versus distance (d_{TR}).

Figure 9 illustrates the comparative study of the performance of proposed optimum coupling tuning over the conventional fixed coupled system (where $k_{ST} = 0.1231$ and $k_{RD} = 0.1284$ were set during measurement by keeping both d_{ST} and d_{RD} equal to 7 cm) at 17.1 MHz. The S-parameter and efficiency curves are plotted at various coupling distance d_{TR} for both the simulation and experimental analysis. As observed in both figures, the fixed coupled system suffers from low $|S_{21}|$ and PTE for d_{TR}<25cm due to the split of frequencies which causes the mismatch between source and load impedances at the original resonant frequency. Hence, in line to Equations (23) and (20), the couplings k_{ST} and k_{RD} need to increase for adequate matching at this region. To achieve the maximum PTE for 10cm $\leq d_{TR} \leq$ 25cm, the extracted optimum couplings are found in the range of $0.252 \geq k_{ST}, k_{RD} \geq 0.131$ and practically implemented by adjusting both d_{ST} and d_{RD} approximately within 1.8–7 cm, respectively. When the distance d_{TR} increases over 25 cm, the weak coupling value of k_{TR} rapidly reduces the power transfer capability of the system again. Now at this stage, both k_{ST} and k_{RD} should be decreased to satisfy the matching conditions. In reference to the measured values of k_{TR} for 25cm $\leq d_{TR} \leq$ 85cm, the tunable optimum coupling coefficients and distances are obtained around $0.131 \geq k_{ST}, k_{RD} \geq 0.029$ and 7cm $\leq d_{ST}, d_{RD} \leq$ 16cm. The resultant optimum coupling values and distances correlated to the maximum transfer efficiency are plotted in Figure 8(a) and b), respectively. Even though, the higher value of d_{ST} and d_{RD} typically dictates the loops and intermediate coils to be weakly coupled to each other, but in actual significantly helps to increase the operating range of the resonant coupled WPT system observed in Figure 9.

The results in Figure 9 experimentally validate the effectiveness of the conceptual tunable impedance matching technique, and results more than 10 dB improvements for the extracted S_{21} parameter at both strong and weak coupling regions (Figure 9(a)). The plot illustrates that the PTE reaches high up to 85% without adjusting the source frequency. About, 15.1% and 19.9% of efficiency enhancement are also observed at the corresponding distances of 10 and 70 cm depicted in Figure 9(b). As seen, the measured PTE curve follows a similar pattern to that of the measured magnitude of S_{21}. Compared to the simulation, 3–12% deviation has occurred in

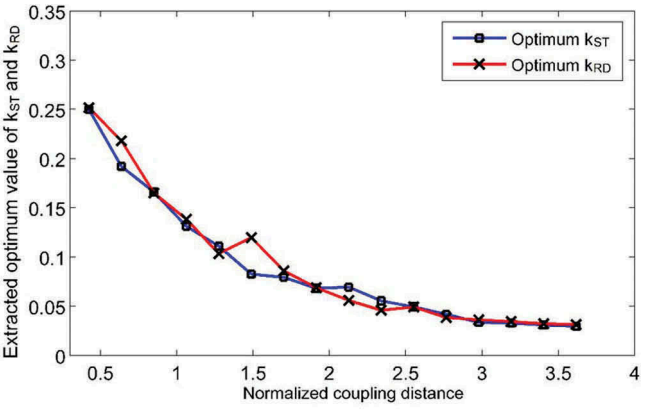

(a)

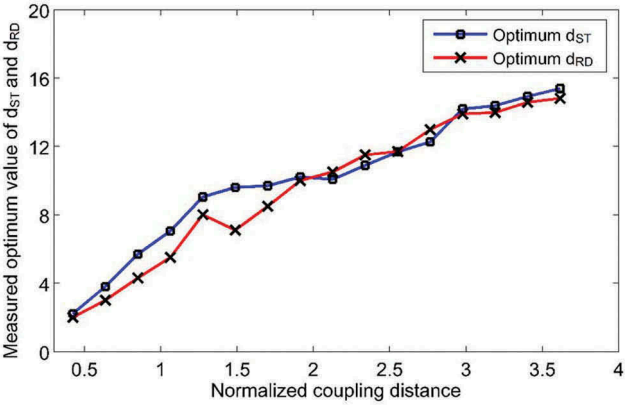

(b)

Figure 8. (a) Extracted optimum coupling coefficients and (b) measured optimum distances as a function of normalised coupling distance.

measured values due to the radiation and conductive losses of the components used in the system. After tuning both the coupling coefficients, the measured waveforms of the input voltage V_{in} and the output voltage V_L for the WPT system are also shown in Figure 10.

The fixed coupled system either operating at strong or weak coupling regions except the critical point causes the system's efficiency to decrease. This is due to the mismatch of input and output impedances with the corresponding optimum source and load impedances illustrated in Figure 11(a). As seen for strong k_{TR}, the normalised input (R_{in}/R_G) and output (R_{out}/R_L) impedance ratios of the fixed coupled system are small and generally less than 1, while $R_{in}/R_G >> 1$ and $R_{out}/R_L >> 1$ are observed at the weaker value of k_{TR}. As the overall circuit impedance of the resonant coupled system varies with a function of $1/k_{TR}^2$, neither tuning of k_{ST} (keeping k_{RD} fixed) nor k_{RD} (keeping k_{ST} fixed) ensure the impedance matching on both the input and output sides for maximum PTE as observed in Figure 11(a). In contrast, the optimum tuning of both k_{ST} and k_{RD} together in Equations (23) and (20) approximately provides the unity normalised impedance value, and assures the satisfactory matching at both sides of the system. A little deviation at close distances observed in the plot is due to the strong parasitic cross-coupling effects. Figure 11(b) also demonstrates the need of optimum tuning of k_{ST} and k_{RD} together to enhance S_{21} for maximum power gain.

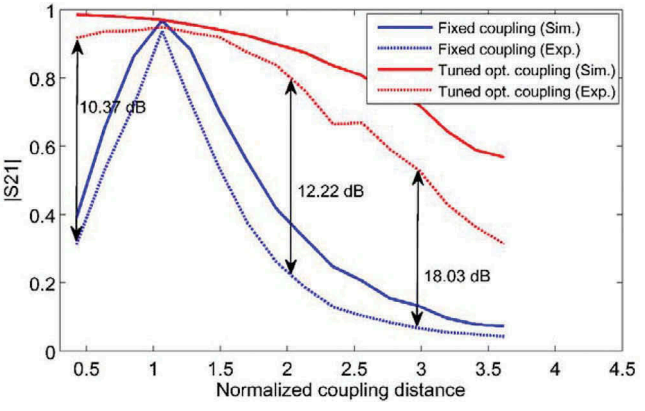

(a)

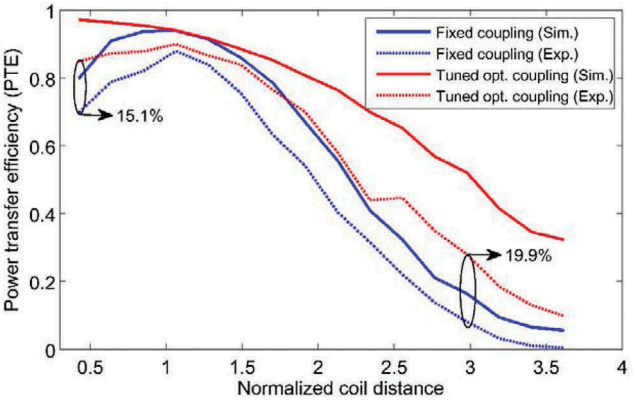

(b)

Figure 9. Simulated and experimental results of (a) $|S_{21}|$ and (b) power transfer efficiency of the resonant coupled WPT using optimum coupling tuning plotted as a function of normalised coupling distance (The normalised coil distance is measured as the ratio of d_{TR} to mean diameter of TX/RX coil).

Furthermore, the proposed tunable matching also successfully conserves the resonant frequency and reduces the power reflection in resonant coupled WPT graphically demonstrated in Figure 12. The figure shows the frequency characteristics of the power reflection ratio (PRR) and power transmission ratio (PTR) of the system to explain the relationship between the power reflection and frequency. The PRR and PTR used for EM field analysis were calculated from the following relations (Imura & Hori, 2011)

$$PRR = |S_{11}|^2 \times 100[\%] \tag{26}$$

$$PTR = |S_{21}|^2 \times 100[\%], \tag{27}$$

where S_{11} and S_{21} represent the wave reflection and transmission coefficients, respectively. From the graphs, it is observed that the lower value of PTE in fixed coupled system confirms the degradation of the magnitude of power transfer to the load (Figure 12(a-i) and Figure 12(b-i)). On the other hand, the coupling tuning not only compensate the splitting of resonant frequency but also decrease the power reflection (ended up within 5–8% of efficiency gap during the experiment) for high efficiency shown in Figure 12(a-ii) and Figure 12(b-ii), respectively.

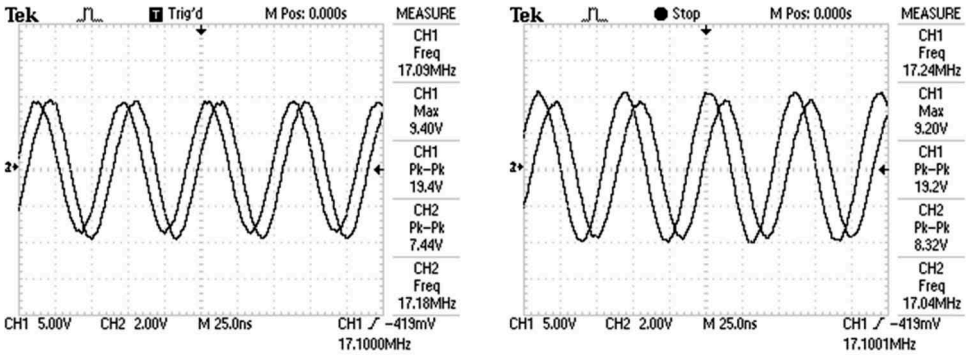

(i) At fixed coupling (ii) At optimum coupling

(a) Coupling distance, d_{TR} = 20 cm

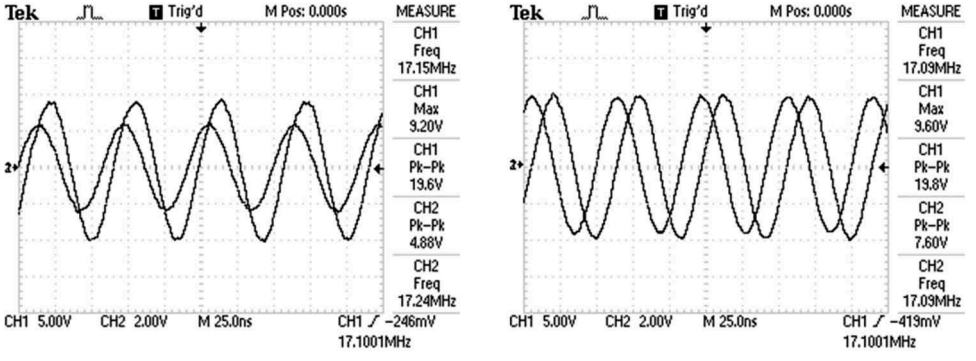

(i) At fixed coupling (ii) At optimum coupling

(b) Coupling distance, d_{TR} = 35 cm

Figure 10. The measured waveforms of input and output voltages for resonant coupled WPT system operating at (i) fixed coupling and (ii) optimum coupling for distance (a) d_{TR}= 20 cm and (b) d_{TR}= 35 cm.

Figure 13 compares the proposed tunable impedance matching with the techniques of frequency tracking (Dukju & Songcheol, 2013b; Sample et al., 2011) and L-matching using LC filter circuits (Teck Chuan et al., 2013; Waters et al., 2012, August) for maximum transfer efficiency. For optimum frequency tracking, the source frequency is selected based on the maximum efficiency point, whereas tunable LC filter circuits are used at both TX and RX sides for L-matching method. Both these techniques are practically implemented with the designed coil over 10–85 cm coupling distance. As seen in graph, the LC circuit improves efficiency than the fixed coupled system, whereas the frequency tracking approach is effective only at strong coupling regimes. Compared to these two techniques, the proposed matching with optimum coupling tuning provides decent improvements in efficiency of more than 5–10%. In some cases, the coupling tuning provides lower efficiency than the LC circuit which may because of the effects of parasitic cross-coupling and capacitive detuning.

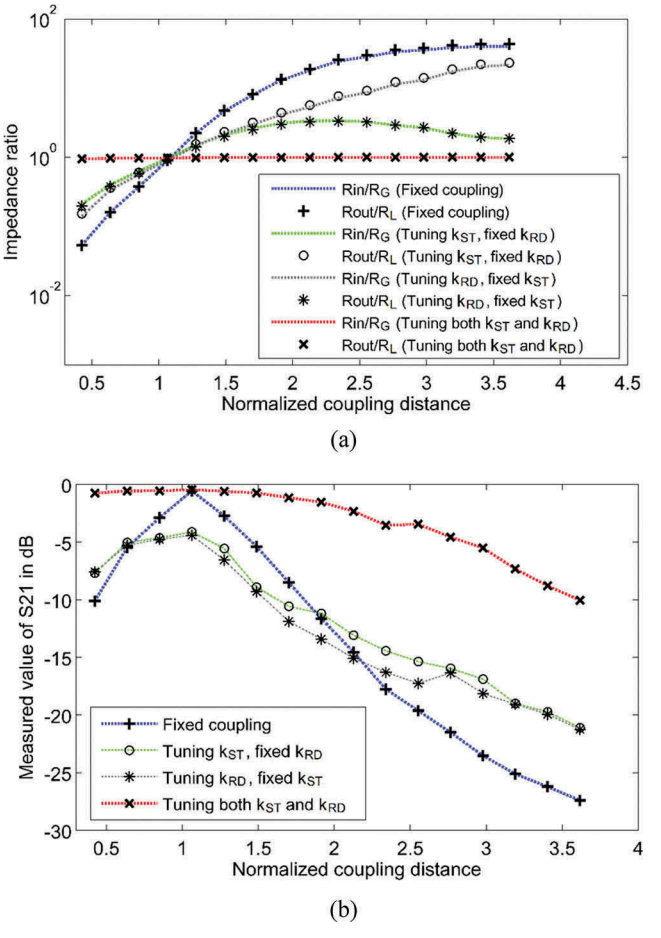

Figure 11. (a) Normalised input–output impedance ratio plot and (b) S_{21} in dB at different coupling arrangements in WPT.

5. Conclusion

The WPT circuit impedances are highly affected by the change of couplings between resonant coupled coils and, thereby, often shift the resonant point and decrease the transfer efficiency at large scale. Therefore, a practical WPT system using impedance matching technique must uphold the resonant point to achieve optimum PTE. In this work, an impedance matching technique based on optimum coupling tuning is presented to enhance the efficiency of the resonant coupled WPT system. Design methodologies and empirical matching equations with proposed technique for the optimum power transfer are derived from the perspective of lumped circuit model.

The effect of the proposed matching technique is validated through simulation and experiment, and compared with the conventional fixed coupled WPT system. The experimental verification indicates the increase of PTE over 80% at fixed operating frequency within extended operating range. The measurement shows 15.1% and 19.9% improvements on efficiency at a distance of 10 and 70 cm, respectively, and over 10 dB improvement in S_{21} parameter. Moreover, the proposed optimum coupling tuning successfully compensate the frequency shifting effects as well as confirms the adequate matching at both sides of the resonant coupled system. The implemented system results in being much more effective compared to prior works based on frequency tracking and tunable LC circuits, and could enable industries to practically implement highly efficient cordless charging system for future portable electronic devices.

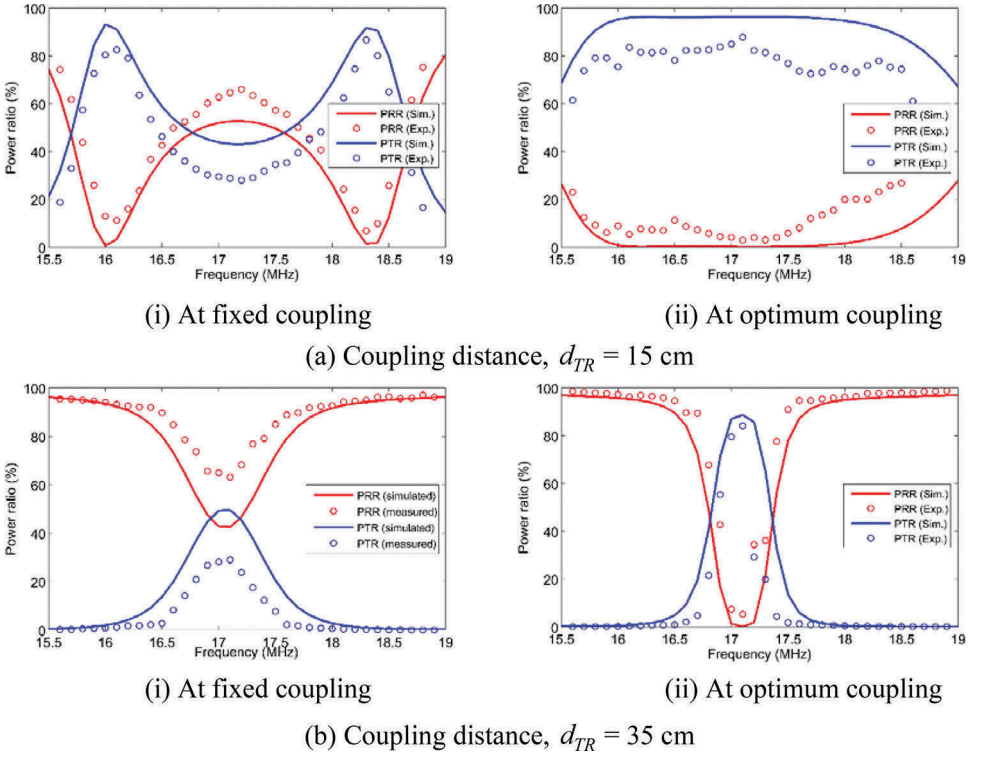

Figure 12. Frequency characteristics of the WPT system operating at (i) fixed coupling and (ii) optimum coupling for distance (a) d_{TR}= 15 cm and (b) d_{TR}= 35 cm.

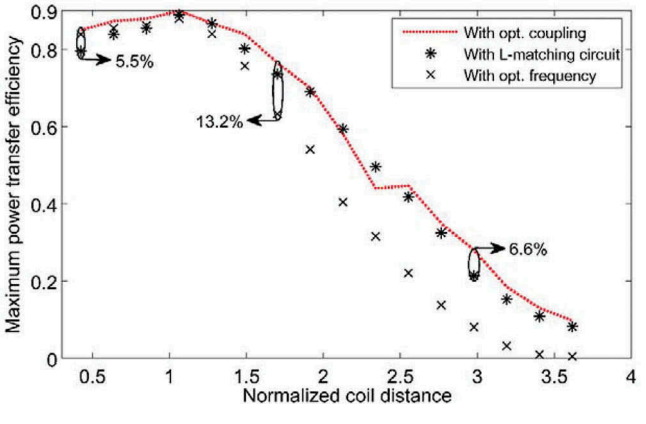

Figure 13. Efficiency comparison of optimum coupling tuning with frequency tracking and L-matching techniques.

Acknowledgements

This research work is supported by the University of Malaya High Impact Research (HIR) Grant (UM.C/628/HIR/ENG/51) sponsored by the Ministry of Higher Education (MOHE), Malaysia.

Disclosure statement

No potential conflict of interest was reported by the authors.

Funding

This research work is supported by the University of Malaya High Impact Research (HIR) Grant (UM.C/628/HIR/ENG/51) sponsored by the Ministry of Higher Education (MOHE), Malaysia.

References

Abbasi, M. I., Atif Adnan, S., Amin, M., & Kamran, F. (2009, January). Wireless power transfer using microwaves at 2.45 GHz ISM band. In Proceedings of Sixth International Bhurban Conference on applied sciences and technology (pp. 99–102). Islamabad: IEEE.

Barman, S. D., Reza, A. W., Kumar, N., & Anowar, T. I. (2016). Two-side impedance matching for maximum wireless power transmission. *IETE Journal of Research*, *62*(4), 532–539. doi:10.1080/03772063.2015.1117954

Barman, S. D., Reza, A. W., Kumar, N., Karim, M. E., & Munir, A. B. (2015, November). Wireless powering by magnetic resonant coupling: Recent trends in wireless power transfer system and its applications. *Renewable and Sustainable Energy Reviews*, *51*, 1525–1552. doi:10.1016/j.rser.2015.07.031

Benford, J. (2008, June). Space applications of high-power microwaves. *IEEE Transactions on Plasma Science*, *36*(3), 569–581. doi:10.1109/TPS.2008.923760

Brown, W. C., & Eves, E. E. (1992, June). Beamed microwave power transmission and its application to space. *IEEE Transactions on Microwave Theory and Techniques*., *40*(6), 1239–1250. doi:10.1109/22.141357

Casanova, J. J., Zhen Ning, L., & Jenshan, L. (2009, August). A loosely coupled planar wireless power system for multiple receivers. *IEEE Transactions on Industrial Electronics*, *56*(8), 3060–3068. doi:10.1109/TIE.2009.2023633

Chen, C. J., Chu, T. H., Lin, C. L., & Jou, Z. C. (2010, July). A study of loosely coupled coils for wireless power transfer. *IEEE Transactions on Circuits and Systems - II: Expres Briefs*, *57*(7), 536–540. doi:10.1109/TCSII.2010.2048403

Choi, S. Y., Gu, B. W., Jeong, S. Y., & Rim, C. T. (2015, March). Advances in wireless power transfer systems for roadway-powered electric vehicles. *IEEE Journal of Emerging and Selected Topics in Power Electronics*, *3*(1), 18–36. doi:10.1109/JESTPE.2014.2343674

Dukju, A, & Songcheol, H. (2013a, January). A study on magnetic field repeater in wireless power transfer. *IEEE Transactions on Industrial Electronics*, *60*(1), 360–371. doi: 10.1109/TIE.2012.2188254

Dukju, A, & Songcheol, H. (2013b, July). Effect of coupling between multiple transmitters or multiple receivers on wireless power transfer. *IEEE Transactions on Industrial Electronics*, *60*(7), 2602–2613. doi: 10.1109/TIE.2012.2196902

Dukju, A., & Songcheol, H. (2014, March). A transmitter or a receiver consisting of two strongly coupled resonators for enhanced resonant coupling in wireless power transfer. *IEEE Transactions on Industrial Electronics*, *61*(3), 1193–1203. doi:10.1109/TIE.2013.2257151

Hao, J., Junmin, Z., Di, L., Chao, K. K., Shyshenq, L., Shahnasser, H., … Roy, S. (2013, August). A low-frequency versatile wireless power transfer technology for biomedical implants. *IEEE Transactions on Biomedical Circuits and Systems*, *7*(4), 526–535. doi:10.1109/TBCAS.2012.2220763

Hatanaka, K., Sato, F., Matsuki, H., Kikuchi, S., Murakami, J., Kawase, M., & Satoh, T. (2002, September). Power transmission of a desk with a cord-free power supply. *IEEE Transactions on Magnetics*, *38*(5), 3329–3331. doi:10.1109/TMAG.2002.803120

IEEE Standards Coordinating Committee 28, on Non-ionizing Radiation Hazards. (2006, April). IEEE standard for safety levels with respect to human exposure to radio frequency electromagnetic fields, 3 kHz to 300 GHz. New York: Institute of Electrical and Electronics Engineers, Incorporated.

Imura, T., & Hori, Y. (2011, October). Maximizing air gap and efficiency of magnetic resonant coupling for wireless power transfer using equivalent circuit and Neumann formula. *IEEE Transactions on Industrial Electronics*, *58*(10), 4746–4752. doi:10.1109/TIE.2011.2112317

Jabbar, H., Song, Y. S., & Jeong, T. T. (2010, February). RF energy harvesting system and circuits for charging of mobile devices. *IEEE Transactions on Consumer Electronics*, *56*(1), 247–253. doi:10.1109/TCE.2010.5439152

Jang, Y. J., Suh, E. S., & Kim, J. W. (2016, June). System architecture and mathematical models of electric transit bus system utilizing wireless power transfer technology. *IEEE Systems Journal*, *10*(2), 495–506. doi:10.1109/JSYST.2014.2369485

Karalis, A., Joannopoulos, J. D., & Soljačić, M. (2008, January). Efficient wireless non-radiative mid-range energy transfer. *Annals of Physics*, *323*(1), 34–48. doi:10.1016/j.aop.2007.04.017

Kiani, M., & Ghovanloo, M. (2012, September). The circuit theory behind coupled-mode magnetic resonance-based wireless power transmission. *IEEE Transactions on Circuits and Systems - I: Regular Papers*, *59*(9), 2065–2074. doi:10.1109/TCSI.2011.2180446

Kim, J., Choi, W. S., & Jeong, J. (2013). Loop switching technique for wireless power transfer using magnetic resonance coupling. *Progress in Electromagnetics. Research*, *138*, 197–209. doi:10.2528/PIER13012118

Kurs, A., Karalis, A., Moffatt, R., Joannopoulos, J. D., Fisher, P., & Soljačić, M. (2007). Wireless power transfer via strongly coupled magnetic resonances. *Science*, *317*, 83–86. doi:10.1126/science.1143254

Lu, K., & Nguang, S. K. (2015, May). Design of auto-tuning capacitive power transfer system for wireless power transfer. *International Journal of Electronics*, *103*(9), 1430–1445.

Madawala, U. K., & Thrimawithana, D. J. (2011, October). A bidirectional inductive power interface for electric vehicles in V2G systems. *IEEE Transactions on Industrial Electronics*, *58*(10), 4789–4796. doi:10.1109/TIE.2011.2114312

Moon, Y. K., Park, H. G., Kim, H., Tiwari, H. D., Kim, S., & Lee, K. Y. (2015, February). Wide input range, high-efficiency magnetic resonant wireless power receiver. *International Journal of Electronics*, *102*(2), 326–344. doi:10.1080/00207217.2014.896419

Nair, V. V., & Choi, J. R. (2016, March). An efficiency enhancement technique for a wireless power transmission system based on a multiple coil switching technique. *Energies*, *9*(3), 156. doi:10.3390/en9030156

Park, B. C., & Lee, J. H. (2014, May). Adaptive impedance matching of wireless power transmission using multi-loop feed with single operating frequency. *IEEE Transactions on Antennas and Propagation*, *62*(5), 2851–2856. doi:10.1109/TAP.2014.2307340

Park, H. G., Jang, J. H., Kang, J. H., Tiwari, H. D., Moon, Y. K., & Lee, K. Y. (2014, April). Automatic power controlled, load compensated magnetic resonant wireless power transmitter. *International Journal of Electronics Letters*, *2*(2), 121–133. doi:10.1080/00207217.2014.880991

RamRakhyani, A. K., Mirabbasi, S., & Mu, C. (2011, February). Design and optimization of resonance-based efficient wireless power delivery systems for biomedical implants. *IEEE Transactions on Biomedical Circuits and Systems*, *5*(1), 48–63. doi:10.1109/TBCAS.2010.2072782

Ricketts, D. S, Chabalko, M. J, & Hillenius, A. (2013a, February). experimental demonstration of the equivalence of inductive and strongly coupled magnetic resonance wireless power transfer. *Applied Physics Letters*, *102*(5), 053904. doi: 10.1063/1.4788748

Ricketts, D. S., Chabalko, M. J., & Hillenius, A. (2013b, October). Optimization of wireless power transfer for mobile receivers using automatic digital capacitance tuning. In Proceedings of European Microwave Conference. Nuremberg: 515–518. IEEE

Sallan, J., Villa, J. L., Llombart, A., & Sanz, J. F. (2009, June). Optimal design of icpt systems applied to electric vehicle battery charge. *IEEE Transactions on Industrial Electronics*, *56*(6), 2140–2149. doi:10.1109/TIE.2009.2015359

Sample, A. P., Meyer, D. A., & Smith, J. R. (2011, February). Analysis, experimental results, and range adaptation of magnetically coupled resonators for wireless power transfer. *IEEE Transactions on Industrial Electronics*, *58*(2), 544–554. doi:10.1109/TIE.2010.2046002

Teck Chuan, B., Kato, M., Imura, T., Sehoon, O., & Hori, Y. (2013, September). Automated impedance matching system for robust wireless power transfer via magnetic resonance coupling. *IEEE Transactions on Industrial Electronics*, *60*(9), 3689–3698. doi:10.1109/TIE.2012.2206337

Terman, F. E. (1943). *Radio engineer's handbook*. New York: McGraw-Hill Book Company.

Wang, W., Chen, Y., Yang, S., Chan, A., Wang, Y., & Cao, Q. (2016, February). Design and experiment of wireless power transfer systems via electromagnetic field near-zone region. *International Journal on Electronics*, *29*, 3060–3068.

Waters, B. H., Sample, A. P., & Smith, J. R. (2012, August). Adaptive impedance matching for magnetically coupled resonators. In Proceedings of the PIERS (pp. 694–701), Moscow.

Wei, Z., Siu-Chung, W., Tse, C. K., & Qianhong, C. (2014, June). Analysis and comparison of secondary series- and parallel-compensated inductive power transfer systems operating for optimal efficiency and load-independent voltage-transfer ratio. *IEEE Transactions on Power Electronics*, *29*(6), 2979–2990. doi:10.1109/TPEL.2013.2273364

Yiming, Z., Zhengming, Z., & Kainan, C. (2014, July). Frequency-splitting analysis of four-coil resonant wireless power transfer. *IEEE Transactions on Industrial Applications*, *50*(4), 2436–2445. doi:10.1109/TIA.2013.2295007

Yoon, C. S., Nam, S. S., & Cho, S. H. (2016, April). A rapid multi-device wireless power transfer scheme using an intermediate energy storage. *International Journal of Electronics*, *103*(4), 591–608. doi:10.1080/00207217.2015.1036807

Yungtaek, J., & Jovanovic, M. M. (2003, June). A contactless electrical energy transmission system for portable-telephone battery chargers. *IEEE Transactions on Industrial Electronics*, *50*(3), 520–527. doi:10.1109/TIE.2003.812472

Zhen Ning, L., Chinga, R. A., Ryan, T., & Jenshan, L. (2009, May). Design and test of a high-power high-efficiency loosely coupled planar wireless power transfer system. *IEEE Transactions on Industrial Electronics*, *56*(5), 1801–1812. doi:10.1109/TIE.2008.2010110

Appendix

To verify the accuracy of $Z_{in} = R_G^*$ and $Z_{out} = R_L^*$ via the optimum tuning of k_{ST} and k_{RD}, respectively, the expressions of formulas (20)–(23) from Section 3 are rearranged as following:

$$k_{RD(opt)} = \sqrt{\frac{a}{Q_R Q_D}} \tag{A.1}$$

$$Z_{out} = \omega_0 L_D \left(\frac{k_{RD}^2 Q_R}{a}\right) - R_{PD} \tag{A.2}$$

$$k_{ST(opt)} = \sqrt{\frac{a}{Q_S Q_T}\left(\frac{R_G - R_{PS}}{R_G + R_{PS}}\right)} \tag{A.3}$$

$$Z_{in} = R_{PS} + (R_G + R_{PS})\left(\frac{k_{ST}^2 Q_S Q_T (1 + k_{RD}^2 Q_R Q_D)}{a^2 + k_{RD}^2 Q_R Q_D}\right), \tag{A.4}$$

where $a = \sqrt{1 + k_{TR}^2 Q_T Q_R}$. Using the extracted lumped parameter values given in Table 2, the Q-factor of TX and RX coils are Q_T=913.96 and Q_R=921.94 at the resonant frequency of 17.1 MHz. Similarly, the Q-factor of the source and load coil can be determined with the optimum loading value of R_G and R_L, respectively. The theoretical preciseness of above formulas in adequate impedance matching at the input and output sides of the resonant coupled WPT are demonstrated in tables below for different values of R_G and R_L. As observed, the matching conditions defined in (A.1) and (A.3) approximately able to transform both R_G and R_L to the optimal Z_{in} and Z_{out}, respectively, for different coupling distances (i.e. for different coupling coefficients k_{TR}).

Table A1. Input–output impedance values for Q_S =3.074 and Q_D =3.037 with $R_G = R_L$ =50 Ω.

k_{TR}	$k_{RD(opt)}$ from (A.1)	$k_{ST(opt)}$ from (A.3)	$Z_{out}$from (A.2)	$Z_{in}$from (A.4)
0.1	0.181	0.179	49.98	49.92
0.05	0.128	0.126	49.972	49.52
0.01	0.057	0.057	49.28	49.78
0.005	0.041	0.0405	50.11	50.02
0.001	0.022	0.0218	49.94	50.1

Table A2. Input–output impedance values for Q_S =3.074 and Q_D =14.66 with R_G =50 Ω and R_L =10 Ω.

k_{TR}	$k_{RD(opt)}$ from (A.1)	$k_{ST(opt)}$ from (A.3)	$Z_{out}$from (A.2)	$Z_{in}$from (A.4)
0.1	0.082	0.179	9.9	49.48
0.05	0.058	0.126	9.89	49.04
0.01	0.0261	0.057	9.89	50.2
0.005	0.0186	0.0405	9.29	49.83
0.001	0.01	0.0218	9.95	50.08

Table A3. Input–output impedance values for Q_S =14.825 and Q_D =1.525 with R_G =10 Ω and R_L =100 Ω.

k_{TR}	$k_{RD(opt)}$ from (A.1)	$k_{ST(opt)}$ from (A.3)	$Z_{out}$from (A.2)	$Z_{in}$from (A.4)
0.1	0.255	0.078	99.65	9.83
0.05	0.18	0.055	99.27	9.74
0.01	0.081	0.024	99.9	9.3
0.005	0.0577	0.017	99.72	9.17
0.001	0.031	0.0095	99.61	9.8